Smith, P. R., Jardine, R. J. & Hight, D. W. (1994). *Géotechnique* **44**, No. 2, 359–362

DISCUSSION

The yielding of Bothkennar clay

P. R. SMITH, R. J. JARDINE and D. W. HIGHT (1992). *Géotechnique* **42**, No. 2, 257–274

S. J. Wheeler and G. T. Houlsby, *University of Oxford*

This discussion concerns the variation with drained stress path direction θ of the bulk stiffness K' and shear stiffness G of Bothkennar clay as reported by the Authors in Figs 12 and 13.

Secant and tangent values of K' and G were back-calculated by the Authors from the applied stress increments $\delta p'$ and δq and the measured increments of volumetric strain $\delta\varepsilon_{vol}$ and shear strain $\delta\varepsilon_s$, assuming isotropic elastic behaviour

$$\begin{bmatrix} \delta p' \\ \delta q \end{bmatrix} = \begin{bmatrix} K' & 0 \\ 0 & 3G \end{bmatrix} \begin{bmatrix} \delta\varepsilon_{vol} \\ \delta\varepsilon_s \end{bmatrix} \tag{2}$$

The variation of normalized bulk stiffness K'/p' with stress path direction $\theta = \tan^{-1}(\delta q/\delta p')$, presented in Fig. 12, shows K' tending to zero as θ approaches 90° or 270° when $\delta p'$ is zero. This reduction of K' to zero is an inevitable consequence of equation (2) if there are any volumetric strains for stress paths where the mean effective stress p' remains constant. Such volumetric strains will occur either if the material is anisotropic or if there are plastic components of strain. Similarly, the reduction towards zero of normalized shear stiffness G/p' as θ approaches zero, which can be observed in the experimental data presented in Fig. 13 (except for the low strain secant value curve), is a consequence of equation (2) if, for stress paths where the deviator stress q remains constant, there are any shear strains due to anisotropy or plastic behaviour. The shear stiffness would also be expected to tend to zero at $\theta = 180°$, but the Authors state in Fig 13 that no data are available at this value of θ.

As the reduction to zero of K' (at $\theta = 90°$ and 270°) and G (at $\theta = 0°$) shown in Figs 12 and 13 could be attributed to anisotropy, a question which arises is whether the entire variation of K' and G with θ observed by the Authors can be explained simply by anisotropic elastic behaviour, or whether the apparent variation of bulk and shear stiffness with stress path direction was caused by something else, such as plastic behaviour.

Graham and Houlsby (1983) showed that, for the restricted conditions of a triaxial test, the stress–strain relations of a cross-anisotropic (transversely isotropic) elastic material may be given by

$$\begin{bmatrix} \delta p' \\ \delta q \end{bmatrix} = \begin{bmatrix} K^* & J \\ J & 3G^* \end{bmatrix} \begin{bmatrix} \delta\varepsilon_{vol} \\ \delta\varepsilon_s \end{bmatrix} \tag{3}$$

where J is a coupling modulus and asterisks have been added to the leading diagonal terms in the stiffness matrix to emphasize the fact that the material is no longer isotropic. The stiffness matrix in equation (3) must be symmetric about the leading diagonal because of the thermodynamic requirement that it must be possible to derive the stresses during recoverable elastic behaviour by differentiation of an elastic strain energy potential (see, for example, Love, 1927). The various moduli in the anisotropic stiffness matrix should not be confused with the alternative moduli introduced by authors such as Atkinson, Richardson & Stallebrass (1990), the inverse of which are terms in the compliance matrix.

If the material behaviour is actually governed by the anisotropic elastic relations of equation (3), but the measured strains are interpreted in terms of isotropic elastic behaviour (equation (2)), then the apparent bulk and shear moduli K_{eq} and G_{eq} will vary with stress path direction θ, as stated by Graham & Houlsby (1983)

$$K_{eq} = \frac{3K^*G^* - J^2}{3G^* - J\tan\theta} \tag{4}$$

$$G_{eq} = \frac{3K^*G^* - J^2}{3(K^* - J/\tan\theta)} \tag{5}$$

Figures 28 and 29 show the variation with θ of normalized equivalent bulk and shear stiffness K_{eq}/p' and G_{eq}/p' predicted by equations (4) and (5), together with the corresponding experimental values from the drained probing tests reported by the Authors (abstracted from Figs 12 and 13). The experimental points shown are tangent values (because the Authors presented only fitted curves for secant values and not actual data points) at the lowest strain of 0·01%, where the behaviour is most likely to be elastic.

The theoretical curves shown in Figs 28 and 29 were constructed by assuming the following values for the normalized anisotropic elastic

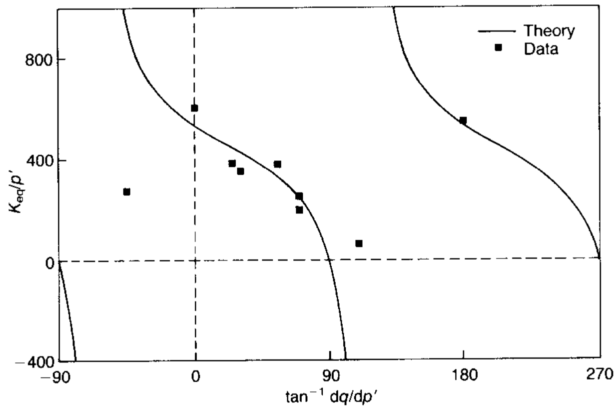

Fig. 28. Variation of normalized equivalent bulk stiffness K_{eq}/p' with stress path direction

moduli: $K^*/p' = 840$, $G^*/p' = 560$ and $J/p' = -720$. The negative value of coupling modulus J implies that the material was stiffer horizontally than vertically, and the particular values chosen correspond to a ratio of horizontal to vertical stiffness α^2 of 4·08 and an anisotropic Poisson's ratio ν^* of 0·152 (as defined by Graham & Houlsby, 1983). The values of K^*/p', G^*/p' and J/p' were optimized only very crudely to fit the experimental data (using subjective judgement) because, as discussed below, there were very good reasons why some of the data points would not be expected to fit the theoretical curves, and therefore unequal weighting would need to be applied to the different data points in any rigorous optimization exercise.

Figure 28 shows that, with the exception of the data points at $\theta = 315°$ and $\theta = 110°$, the theoretical values of K_{eq}/p' predicted by equation (4) are within 15% of the measured values and that the substantial reduction in K_{eq}/p' between $\theta = 0$ and $\theta = 90°$ is modelled correctly. Fig. 28 also suggests a possible explanation for the lack of fit between predicted and observed values of K_{eq}/p' at $\theta = 315°$ and $\theta = 110°$. At these two values of θ equation (4) predicts extremely high values of K_{eq}, suggesting very small volumetric strains, because the predicted components of volumetric strain due to changes in p' and q are of opposite sign and almost equal magnitude. The experimental values of K_{eq}/p' were, however, measured at a fixed volumetric strain of 0·01%. If the elastic components of volumetric strain were extremely small (as predicted by the anisotropic model), then volumetric strains of 0·01% could be achieved only by loading beyond yield into the plastic region, at which point the tangent stiffness recorded in Fig. 28 would drop to a much lower

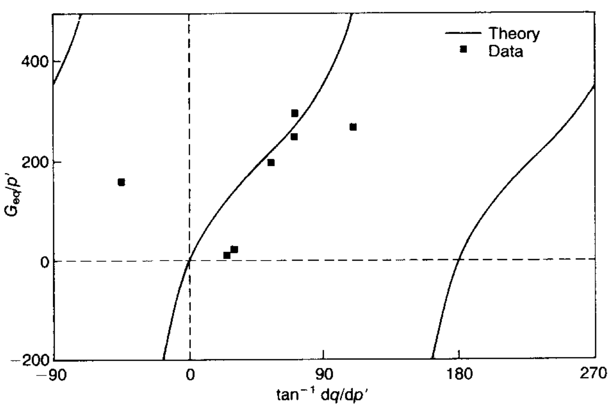

Fig. 29. Variation of normalized equivalent shear stiffness G_{eq}/p' with stress path direction

value. It would be useful to examine values of K_{eq}/p' measured at a fixed size of stress increment vector $\sqrt{(\Delta p^2 + \Delta q^2)}$, sufficiently small to avoid yield, to see whether or not these measurements showed better agreement with predicted values over the full range of stress path directions than values of K_{eq}/p' measured at a fixed volumetric strain.

Figure 29 shows that the predicted values of normalized equivalent shear modulus G_{eq}/p' are in reasonable agreement (less than 15% error) with measured values for the three data points with $\theta = 55°$ or $\theta = 70°$. Large discrepancies are again observed at $\theta = 315°$ and $\theta = 110°$, where the predicted values of G_{eq}/p' are extremely high. This is consistent with the suggestion that, in order to achieve a shear strain of 0·01% (the point at which values of G_{eq} were measured), it was necessary, at these values of θ, to load into the plastic range because elastic components of shear strain were extremely small. More surprisingly, lack of fit between predicted and measured values of G_{eq}/p' is observed at $\theta = 25°$ and $\theta = 30°$ (where the predicted values of G_{eq}/p' are relatively low). However, Fig. 13 shows that these data points correspond to a region where the secant values of G_{eq}/p' were very high, whereas the tangent values were very low (described by the Authors as anomalous behaviour). Such a pattern would be produced if the soil were strained beyond yield into the plastic region.

A simple isotropic elastic model is therefore able to reproduce some of the observed variation of apparent bulk and shear stiffness with stress path direction. Remaining anomalies may be partly the result of loading beyond the elastic range in tests conducted at certain values of θ. This possibility could be investigated by plotting values of apparent bulk and shear stiffness measured at a fixed size of stress increment vector rather than values measured at fixed increments of volumetric or shear strain.

One feature of the observed behaviour that is not well represented by an anisotropic elastic model is the slope of the effective stress path recorded in the undrained triaxial compression and extension tests. The anisotropic model predicts stress paths inclined at an angle given by $\tan \theta = 3G^*/J$ (Graham & Houlsby, 1983). For a material which is stiffer horizontally than vertically (as suggested by the observed variation of K_{eq}/p' and G_{eq}/p' with θ), the value of J is negative and the stress paths predicted for undrained tests are rotated anticlockwise from the vertical (at $\theta = 113°$ and $\theta = 293°$ for the values of G^*/p' and J/p' used to plot the theoretical curves in Figs 28 and 29). Unfortunately the stress paths observed in the undrained tests were rotated slightly clockwise from the vertical (see Fig. 5). A possible cause for this could be incomplete saturation of the samples, as even very small quantities of undissolved air would cause significant compressibility of the pore fluid and hence substantial clockwise rotation of the stress path in undrained tests (Houlsby, Wroth & Wood, 1982).

Authors' reply

The experiments on Bothkennar clay described in the Paper provided new information on the behaviour of a natural soft clay. As data interpretation may be approached from several different standpoints, the Authors intended the Paper to provide sufficient information to allow others to re-examine the experiments.

Figures 12 and 13 were included to show, in a reasonably compact form, how the secant and tangent values of $(\Delta q/\Delta 3\varepsilon_s)/p'$ and $(\Delta p'/\Delta\varepsilon_{vol})/p'$ observed in suites of drained and undrained probing tests changed with stress path direction θ and the level of the strains ε_s and ε_{vol}. Although the two stiffness measures were termed G/p' and K'/p', the Paper states that intact Bothkennar clay has a very small linear elastic range, and that behaviour may be anisotropic even within this region.

It may be seen from Figs 7–10 that the data presented in Figs 12 and 13 are taken from test stages which passed beyond the linear elastic envelope, termed the Y_1 yield surface. Indeed, most of the data points plotted represent test stages where the limit to irrecoverable straining (the Y_2 yield surface) had also been exceeded. Behaviour within this region can be strikingly inelastic (see, for example, Fig. 11).

The Writers propose a simplified cross-anistropic linear elastic stiffness matrix as an alternative way of expressing some of the stiffness data. They obtained the coefficients for their matrix by combining the tangent G/p' data given in Fig. 12 for the $\varepsilon_s = 0{\cdot}01\%$ case with the tangent K'/p' data in Fig. 13 for the $\varepsilon_{vol} = 0{\cdot}01\%$ case. They show that such an expression can mimic some of the trends seen experimentally, and point out that the stiffness minima shown in Figs 12 and 13 can be understood in terms of simple, linear, cross-coupling.

However, there are anomalies between the Writers' simple model and the experimental data. We agree that the principal reason for the divergences between theory and measurements shown in Figs 28 and 29 is that the soil's response is niether linear, nor elastic, over the strain ranges considered. By definition, no single set of matrix coefficients can fit the data beyond the Y_1 surface. As the Writers imply, the matrix terms need to vary with a generalized measure of stress which combines changes in p' and q. Alternatively, generalized strains* may be used which account for $\Delta\varepsilon_s$ and $\Delta\varepsilon_{vol}$. The shapes of the stiffness–strain curves in Figs 9 and 10 vary in different ways with θ, and so simple scalar changes to a single base matrix would not be sufficient. However, it would seem less promising to extend the Writers' elastic approach to deal with non-linearity than to develop a model based on plasticity theory.

The Writers also suggest that the lack of agreement between their simplified model and the measurements of the undrained effective stress path directions may be related to inadequate sample saturation in the experiments. This is improbable because Smith (1992) took particular care to ensure full saturation. Values of B exceeding 0·95 were obtained during initial saturation in every case. The degree of saturation improved further during the subsequent two-week re-consolidation process in which each sample retraced the path shown in Fig. 3, while being subjected to a 300 kPa back pressure and being surrounded by a large volume of de-aired water.

It is far more likely that the effective stress path discrepancy reflects the fundamental shortcomings of linear elastic soil models. For the Writers' model, the effective stress path slope depends solely on the ratio of two fixed matrix terms: $\tan\theta = 3G^*/J$. However, as described, these coefficients are only fixed within the minuscule Y_1 envelope. What is remarkable is that the four undrained tests reported in Fig. 5 show virtually identical effective stress path inclinations $\Delta q/\Delta p'$ from the in situ stress condition until the Y_3 yield surface is engaged, whereas the tangent values of G^* fall by three orders of magnitude over the same stress ranges (Fig. 7). Other experiments by Smith (1992) prove that the undrained effective stress path directions are related systematically to the samples' consolidation histories, rather than to any fixed stiffness anisotropy. In the Authors' experience the ratios of $\Delta q/\Delta p'$ observed in undrained tests on most soil types remain practically constant within their large scale Y_3 yield envelopes. This means that the gradients of the plastic potentials applying in the undrained stress states may be more or less parallel between the Y_1 and the Y_3 surfaces.

* See the sections of the Paper which describe the shape of the Y_2 yield surface, or Simpson (1992).

REFERENCES

Atkinson, J. H., Richardson, D. & Stallebrass, S. E. (1990). Effect of recent stress history on the stiffness of overconsolidated soil. *Géotechnique* **40,** No. 4, 531–540.

Graham, J. & Houlsby, G. T. (1983). Anisotropic elasticity of a natural clay. *Géotechnique* **33,** No. 2, 165–180.

Houlsby, G. T., Wroth, C. P. & Wood, D. M. (1982). Predictions of the results of laboratory test on a clay using a critical state model. *Proceedings of international workshop on constitutive relations for soils, Grenoble* (eds G. Gudehus, F. Darve & I. Vardoulakis), pp. 99–121. Rotterdam: Balkema.

Love, A. E. H. (1927). *A treatise on the mathematical theory of elasticity,* 4th edn. Cambridge University Press.

Simpson, B. (1992). Retaining structures—displacement and design. *Géotechnique* **42,** No. 4, 539–576.

Smith, P. R. (1992). *Properties of high compressibility clays with reference to construction on soft ground.* PhD thesis, University of London.